Multibarrier-tunneling invisible systems

Sergio Cordero[1] and Gastón García-Calderón[2,*]

[1]*Instituto de Ciencias Nucleares, Universidad Nacional Autónoma de México Apartado Postal 70-543, México 04510, D.F., Mexico*

[2]*Instituto de Física, Universidad Nacional Autónoma de México, Apartado Postal 20 364, 01000 México, D.F., Mexico*

(Received 28 August 2014; published 1 December 2014)

Multibarrier-tunneling invisible systems may be formed by a finite chain of building blocks that are tunneling invisible. Here we study these systems as a function of the energy and of the distance among building blocks. We find that the transmission coefficient exhibits a very complex behavior both around unity transmission and near the border of energy gaps. Yet, tunneling invisibility remains for a broad range values of these parameters. We investigate on the relationship of the energy spectra in these systems with the corresponding distribution of the complex poles of the transmission amplitude on the energy plane, in particular with the formation of energy dips and gaps in the transmission spectra. We find that these findings hold also in general for multibarrier resonant tunneling systems.

DOI: 10.1103/PhysRevA.90.062101 PACS number(s): 03.65.Ca, 03.65.Xp, 73.40.Gk

I. INTRODUCTION

An interesting area of investigation on fundamental properties of quantum mechanics has been opened with the possibility of designing and constructing one-dimensional (1D) artificial quantum structures. One of these properties is quantum tunneling. There, the issue of *total transparency* of a tunneling particle has attracted attention over the years. It is well known that tunneling of a particle of a given energy through a potential barrier yields in general a partial transmission. Full transmission may occur in resonant tunneling systems, perhaps the simplest one of them consisting of two barriers with a well in between. There, unity transmission may be achieved at some specific energies, the so-called resonance energies. A similar situation occurs in multibarrier resonant tunneling systems having $N+1$ identical barriers alternating with N identical wells. Here, the resonance levels group themselves in minibands, the number of resonance levels in each miniband being equal to the number of wells in the system [1]. In the stationary regime, the time scale for the tunneling process usually refers to the notions of the *time delay* and the *dwell time* [2].

One also finds in the literature a number of approaches that refer to exactly solvable potentials, usually named *reflectionless* or *transparent* potentials, where the transmission coefficient attains a unity value at all incident energies including the threshold energy [3–6]. A well-known example is the Pöschl-Teller potential well which for very specific values of the potential parameters exhibits unity transmission at all energies [7]. These *reflectionless* potentials, however, exhibit a *time delay* and hence are distinguishable from a free evolving particle. More importantly, however, from a physical point of view, is that *reflectionless* here depends on the precise functional dependence of the potential and hence these potentials might be difficult, if not impossible, to construct.

The above considerations suggest to ask to what extent one may design potential profiles in one dimension, that in addition to be totally transparent to a tunneling particle, cannot be distinguished from a free evolving particle. In recent work we addressed the above question and found that indeed this may be possible by an appropriate choice of the potential parameters in systems that involve a combination of barriers and wells, specifically, barrier-well-barrier systems. The transmission coefficient as a function of energy in these systems rises sharply from zero to unity and remains very close to this value along the tunneling region and up to energies a few times above the barrier height. We find that this is intimately related to the distribution of the complex poles of the transmission amplitude on the complex k plane. In particular, the presence of a bound or antibound poles very near $k=0$ and all complex poles located far from the real k axis. Similarly, the *dwell time*, that provides a measure of the time spent within the interaction potential region, yields a value very close to that corresponding to a free evolving particle. We have referred to these systems as *tunneling invisible systems* [8,9]. See also related work in Ref. [10].

Resonant tunneling and tunneling invisibility systems are closely related to each other. One may go from one to the other by modifying appropriately the potential parameters [8]. In resonant tunneling systems the individual barriers are nearly opaque whereas for tunneling invisibility the opposite holds.

We shall refer to a given tunneling invisible barrier-well-barrier system as a tunneling invisible building block (TIBB). In Ref. [8], we considered multibarrier systems involving a few TIBB's to show that they may exhibit invisibility up to a few times the barrier height. However, we did not investigate in detail the properties of chains having many TIBB's. This is relevant because each TIBB is characterized by a length that repeats itself to form the multibarrier system and this necessarily leads, as is well known, to the occurrence of energy regions where unity transmission is partially or totally suppressed, that is, respectively, to transmission energy dips or gaps.

It is the purpose of this work to investigate the properties of multibarrier-tunneling systems formed by chains of TIBB's. We find that a contour map of the transmission as a function of the energy and the distance among TIBB's, exhibits a very complex behavior that involves regions of tunneling invisibility and energy gaps (Fig. 2). In this work we focus in the formation of energy dips and gaps in the transmission spectra and how they relate to the distribution of poles in the

*gaston@fisica.unam.mx

complex energy plane. In order to understand this we have included in our study multibarrier resonant tunneling systems.

This work is organized as follows. Section II deals with *multibarrier-tunneling invisible systems*, in Sec. III we consider the relationship between the transmission amplitude and the distribution of its complex poles with the help of some model calculations for resonant and invisible tunneling systems. Section IV deals with the *dwell time* in multibarrier-tunneling invisible systems and, finally, Section V provides the concluding remarks.

II. MULTIBARRIER-TUNNELING INVISIBLE SYSTEMS

Let us consider a particle of mass m and energy E impinging, from $x < 0$, on a quantum system characterized by a potential profile $V(x)$ of length L, *i.e.*, $V(x) = 0$ outside the region $0 < x < L$. The Schrödinger equation of the problem reads,

$$\frac{\partial^2}{\partial x^2}\psi(x,k) + [k^2 - U(x)]\psi(x,k) = 0 \qquad (1)$$

where $k^2 = (2m/\hbar^2)E$ and $U(x) = (2m/\hbar^2)V(x)$. As is well known, the solutions outside the interaction region may be written respectively as,

$$\psi(x,k) = \begin{cases} e^{ikx} + \mathbf{r}(k)\, e^{-ikx}, & x < 0 \\ \mathbf{t}(k)\, e^{ikx}, & x \geqslant L \end{cases}, \qquad (2)$$

where $\mathbf{r}(k)$ and $\mathbf{t}(k)$ stand, respectively, for the reflection and transmission amplitudes. We denote by $R(E) = |\mathbf{r}(k)|^2$ and $T(E) = |\mathbf{t}(k)|^2$, the corresponding reflection and transmission coefficients. A convenient procedure to calculate the transmission coefficient in multibarrier-tunneling systems is the well known transfer matrix method.

As discussed in Ref. [8], there are different ways to design tunneling invisible systems. Without loss of generality, we consider as TIBB, a system formed by two barriers with a well in between. In order to keep ourselves on physical grounds we characterize the system by typical parameters of semiconductor heterostructures [11]. We consider an effective electronic mass $m = 0.067\, m_e$, where m_e is the electron mass, and parameters of the potential: barrier heights $V_0 = 0.12$ eV, barrier widths $b_0 = 4.0$ Å, well depth $U_0 = -0.12$ eV, well width $w_0 = 8.0$ Å.

Figure 1 shows the signature of invisibility for the TIBB with the above parameters in the transmission coefficient as a function of energy in units of the barrier heights V_0. One sees that the transmission coefficient rises sharply to an essentially unity value along the tunneling region.

A tunneling invisible multibarrier system may be formed by a chain involving a finite number N_{BB} of TIBBs. Here we shall refer only to the case where the distance among the TIBBs corresponds to a fixed value s. Notice that as the number of N_{BB} increases the system tends to a crystalline system. Notice also that other possibilities of forming the chain would be worth exploring, as random values of s or to choose the values of s according to a specific algorithm as the Fibonacci sequence.

Figure 2 exhibits a contour map of $\log_{10}[1 - T(E)]$ as a function of the energy in units of the barrier height E/V_0 and

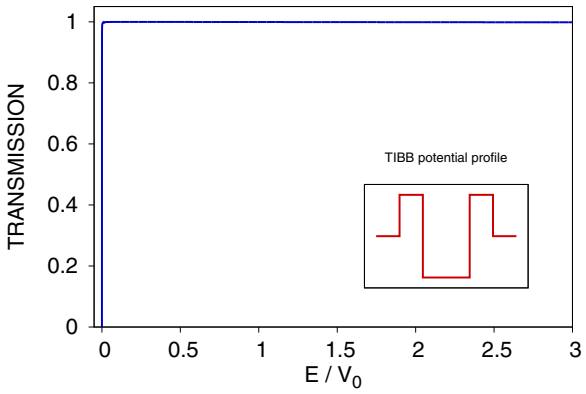

FIG. 1. (Color online) Transmission coefficient as a function of the energy in units of the corresponding potential height V_0 for the tunneling invisible building block (TIBB). The inset shows the TIBB potential profile (see text).

of the distance among the TIBBs in units of the barrier width, s/b_0, for $N_{BB} = 500$. Notice, for the color online figure, that the range of values of $T(E)$ for the yellow, green, blue, and black colors corresponds to values larger than 0.999. Similarly, the white color refers to values of $T(E)$ smaller than 0.999 except the values of wine color that refer to vanishing values of $T(E)$. In addition to the complex patterns shown as a function of s/b_0, it is worth noticing the existence of a large range of values of the distance among TIBBs, $0 \leqslant s/b_0 \lesssim 12$, where tunneling invisibility holds. It is also worth noticing, the appearance of energy gaps where $T(E) \approx 0$. One sees that, as the distance s increases sufficiently, the gaps may appear even within the tunneling region. This resembles a well-known signature of crystalline structures [12]. Although it is not appreciated in the figure, it is worth mentioning that for $s = 0$ the energy gap branches shown in Fig. 2 eventually tend to a finite value of the energy.

Since for a single TIBB there are no energy gaps, one may ask the question of how the energy gaps are formed. We find that a given energy gap requires of a certain number N_{BB} of TIBBs. This is illustrated in Fig. 3, which exhibits a plot

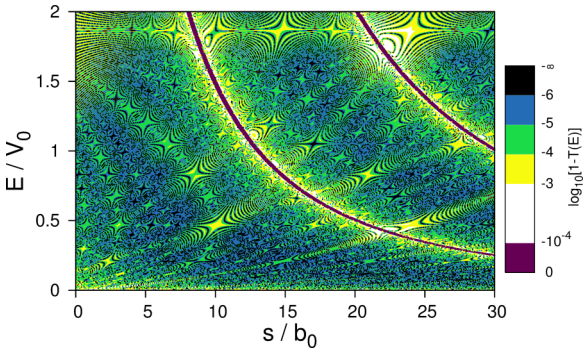

FIG. 2. (Color online) Contour map of $\log_{10}[1 - T(E)]$ as a function of the energy in units of the barrier height, E/V_0, and the distance among TIBBs in units of the barrier width, s/b_0, for a chain of $N_{BB} = 500$ TIBB. The plot shows that for values of $s/b_0 \lesssim 12$ tunneling invisibility holds. Notice that for larger values of s/b_0, a forbidden gap may appear within the tunneling region (see text).

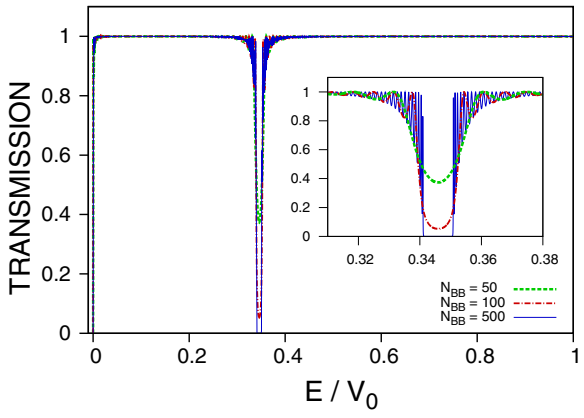

FIG. 3. (Color online) Plot of the transmission coefficient $T(E)$ as a function of the energy in units of the barrier height, E/V_0, and a distance among TIBB $s/b_0 = 25$ for distinct numbers of TIBB, N_{BB} as indicated in the figure. Here the gap band lies inside the tunneling region. Notice that its energy position is independent of N_{BB}. The inset exhibits the structure of the $T(E)$ around the gap band (see text).

of the transmission coefficient as a function of E/V_0 and a fixed value of s, $s_0 = 25b_0$ for systems having a different number of building blocks, $N_{BB} = 50,100,500$, as indicated in the figure. One sees that the energy position where the transmission diminishes to form the energy gap is independent of the number of N_{BB}'s. This is better appreciated in the inset. It is worth emphasizing that as the number of N_{BB}'s diminishes to a single TIBB so does the transmission energy dip which tends essentially to a unity value.

As discussed in detail in Ref. [8], tunneling invisibility follows from a distribution of overlapping resonances corresponding to complex poles of the transmission amplitude. In the next section we investigate the question of the formation of the transmission energy dips and gaps by analyzing the relationship of the transmission spectra with the complex poles of the transmission amplitude.

III. COMPLEX POLES AND TRANSMISSION ENERGY DIPS AND GAPS

We find it convenient to write the transmission amplitude $\mathbf{t}(k)$ in terms of the full outgoing Green's function to the problem, $G^+(x,x';k)$ [1],

$$\mathbf{t}(k) = 2ikG^+(0,L;k)e^{-ikL}. \tag{3}$$

This allows one to obtain a representation for the transmission amplitude as an expansion involving the poles and residues of the outgoing Green's function. This procedure leads exactly to the same results of standard numerical calculations, as the transfer matrix method [11].

It is well known that the function $G^+(x,x';k)$, and hence the transmission amplitude $\mathbf{t}(k)$, possesses an infinite number of complex poles k_n, in general simple, distributed on the complex k plane in a well-known manner [13]. Purely positive and negative imaginary poles $k_n \equiv i\gamma_n$ correspond, respectively, to bound and antibound (virtual) states, whereas complex poles are distributed along the lower half of the k plane. They may be calculated by using iterative techniques as the Newton-Raphson method [14] as discussed, for example, in Appendix B of Ref. [15]. It is worth mentioning that in general there are not approximate analytical expressions for any pole k_n except for distant poles, $k_n \approx n\pi/L - i(2/L)\ln(n)$ with $n \gg 1$ (see also [13]). The outgoing Green's function $G^+(0,L;k)$ may be expanded as an infinite sum in terms of its poles [1,16]. In the case of the transmission spectra of a miniband with well-defined resonant peaks it is only required to take into account the number of poles that correspond to the number of wells of the system [17]. We have recently found, however, that the expansion of $G^+(0,L;k)\exp(-ikL)$ possesses better convergence properties in the presence of strongly overlapping resonances [18], as for tunneling invisibility [8]. It yields the expansion for the transmission amplitude,

$$\mathbf{t}(k) = 2ik\sum_{n=-\infty}^{\infty}\frac{r_n}{k-k_n}e^{-ik_nL}, \tag{4}$$

where r_n follows from the residue of $G^+(x,x';k)$ at the pole k_n [1,19]. It is worth pointing out that for a given energy interval it is sufficient to take into account a finite number of poles. The position of the poles k_n on the complex k plane is a function of both the parameters of the potential and the mass of the particle. Consequently, by varying these parameters the poles follow trajectories along the k plane.

A typical multibarrier resonant tunneling system may be formed by a chain of $N+1$ barriers of height V_0 and width b_0 alternating with N wells of depth $-U_0$ and width w_0. Possibly, the simplest multibarrier resonant tunneling system corresponds to choose $U_0 = 0$. This case leads to the well-known behavior of the transmission coefficient as an alternating succession of energy gaps and minibands, each miniband involving N resonance levels. Using the resonance formalism mentioned above it has been found that the resonance poles of each miniband distribute themselves forming collars on the energy plane [17].

The above considerations suggest analyzing the multibarrier resonant tunneling system, in a similar fashion to the multibarrier invisible system, namely, as a succession of N_{BB} resonant tunneling building blocks (RTBB) that consist of a barrier-well-barrier system. As an example we consider a RTBB with parameters barrier height $V_0 = 0.25$ eV, barrier width $b_0 = 10$ Å, well depth $U_0 = 0$, and well width $w_0 = 50$ Å. Figure 4 displays the transmission coefficient as a function of energy in units of the potential height. Notice that the resonance peak along the tunneling region is broad and overlaps with resonances above the barrier height. The inset to this figure exhibits the corresponding potential profile.

The upper panel in Fig. 5(a) exhibits a plot of the transmission coefficient $T(E)$ as a function of the energy in units of V_0, respectively, for $N_{BB} = 15$ (solid line) and $N_{BB} = 500$ (dense background) with a separation among the RTBBs given by $s_0 = w_0$. Notice that the energy span of the corresponding minibands is independent of the number N_{BB}. In fact, a similar situation occurs for the invisible multibarrier system as shown in the inset to Fig. 3. As a result of the above considerations, it is sufficient to exhibit the distribution of poles of each miniband for the case $N_{BB} = 15$. As shown in the lower panel of Fig. 5(a), the collars have a rounded

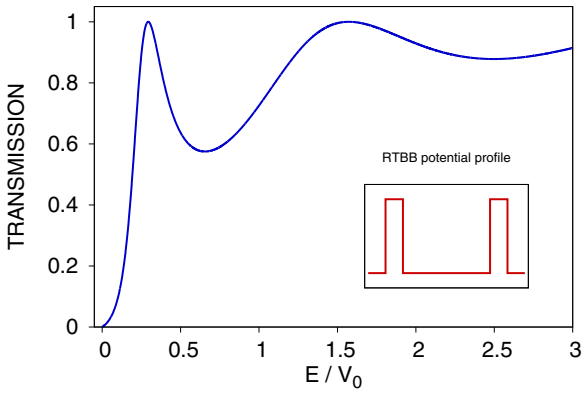

FIG. 4. (Color online) Transmission coefficient as a function of the energy in units of the corresponding potential height V_0 for a resonant tunneling building block (RTBB). The inset shows the RTBB potential profile. See text.

shape. The panels in Fig. 5(b) exhibit a similar situation as in Fig. 5(a), except that $s_0 = 1.4\,w_0$. As may be appreciated, the slight change in the value of s_0 has a dramatic modification for both, the transmission coefficient and the distribution of poles. One sees that each of the previous minibands, with $s_0 = w_0$, splits in two minibands for the case with $s_0 = 1.4\,w_0$, and also, that in the corresponding collars of poles, in addition to the splitting of each of them in two collars, the shape of the second and fourth collars acquire a peaked shape.

Notice that the energy gaps in the transmission spectra shown in the upper panel of Fig. 5(a) subsist, in addition to the new formed gaps described previously, in the upper panel of Fig. 5(b), namely, the first, second, and third gaps of Fig. 5(a) go, respectively, into the first, third, and fifth gaps of Fig. 5(b).

One may obtain a deeper understanding of the origin of these new transmission energy gaps by noticing that the multibarrier resonant tunneling system corresponding to Fig. 5(a), formed by RTBBs, may be also described by a succession of barrier-well (BW) building blocks of length $L_0 = b_0 + w_0$, which in fact constitutes the smallest possible building block for the system. Using this procedure, the system corresponding to Fig. 5(b) may be seen as a succession of barrier-well-barrier-well (BWBW) building blocks where the second well has a width $1.4w_0$ and hence the corresponding length of the building block is $L = 2L_0 + \eta$, with $\eta = 0.4w_0$. Notice that for $\eta = 0$, both systems are identical, however, if $\eta \neq 0$, the length of the smallest building block suffers a dramatic change, namely, it goes from L_0 to $2L_0 + \eta$. In other words, the transmission spectra of the system changes abruptly by modifying slightly a parameter of the system, in this case the parameter s_0.

Since the transmission amplitude is an analytical function of the potential parameters of the system, the previous analysis indicates that by varying gradually the value of the distance from one value of s_0 to another will provoke a gradual splitting of both the transmission spectra characteristics and the corresponding pole distribution. Figure 6 exemplifies this. It exhibits the trajectories of the poles of the first collar in Fig. 5(a) into the first and second collars of Fig. 5(b), by varying the parameter s_0 from $s_0 = w_0$ (circular dots) to $s_0 = 1.4w_0$ (square dots).

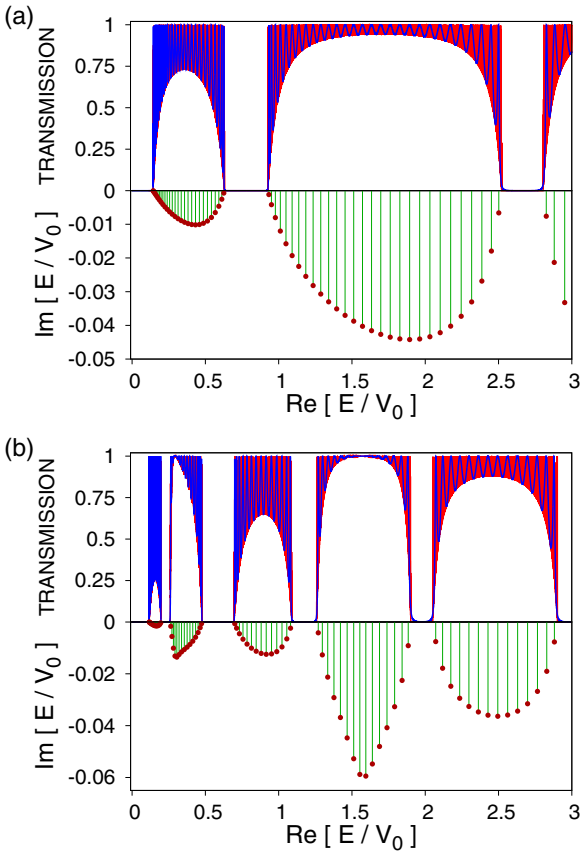

FIG. 5. (Color online) (a) The upper panel exhibits the transmission coefficient as a function of energy in units of the barrier height, respectively, for systems formed with $N_{BB} = 15$ (solid line) and $N_{BB} = 500$ (dense background) resonant tunneling building blocks (RTBB) which are separated by the distance $s_0 = w_0$. One appreciates a succession of allowed and forbidden energy regions which is independent of N_{BB}. The lower panel shows the distribution of complex poles of the transmission amplitude $t(E)$ for $N_{BB} = 15$. They form a collar that distributes itself along each allowed energy region, the number of poles corresponding to the number of unity peaks of $T(E)$, as indicated by the lines joining the poles with the real energy axis. (b) Refers to the case where the RTBB are separated at a distance $s_0 = 1.4w_0$. The upper panel shows that each of the former allowed transmission energy regions splits into two new energy regions. The lower panel exhibits that each of the former collars of poles breaks into two collars, one of them having a peculiar shape (see text).

The changes in the transmission spectra and the pole distribution shown in Figs. 5 and 6 deal with the effect of the parameter s_0, which modifies the total length of the system. One may choose to modify, however, another parameter of the system to obtain similar changes in the transmission spectra. One of these is relevant to understand the energy gaps in multibarrier invisible systems. It consists of a system formed by a chain of TIBBs, as for the invisible system, except that the vanishing depth of the wells U_s corresponding to the separation s among TIBBs acquire a depth U_0. In doing so, the system ceases to be invisible. This may be appreciated by the oscillatory behavior of the transmission coefficient along the tunneling region as shown in the inset to the

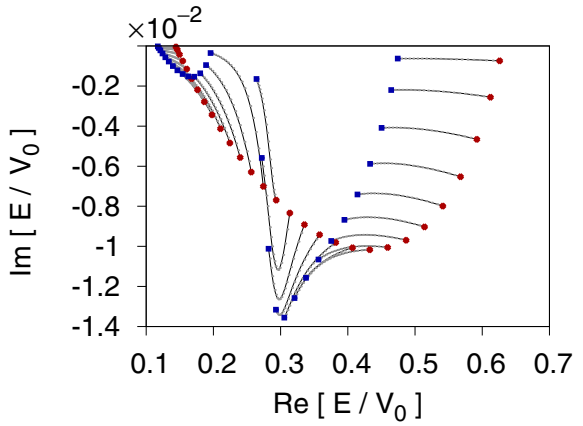

FIG. 6. (Color online) This figure shows the trajectories followed by the poles of the first collar displayed in Fig. 5(a) as a function of the distance between RTBBs from $s_0 = w_0$ (circular dots) to $s_0 = 1.4w_0$ (square dots). One clearly sees that the first collar in Fig. 5(a) goes into the first two collars of Fig. 5(b), showing the formation of the new transmission energy gap (see text).

upper panel of Fig. 7(a). Since the system is not very large, $N_{BB} = 15$, the system exhibits, in a similar fashion as the inset of Fig. 3, a transmission energy dip instead of an energy gap. As shown in the accompanying lower panel to that figure, the pole distribution tends to form a collar. Here, the collar includes also the poles corresponding to bound poles. Taking $U_s = 0$ the tunneling invisible system is restored along the tunneling region, as shown by the transmission spectra exhibited in the inset of the upper panel of Fig. 7(b). One sees, however, in addition to the former energy dip, the apparition of a new transmission energy dip together with the corresponding splitting of the original pole collar into two collars, as displayed in the lower panel to that figure. Clearly by increasing the number of N_{BB}'s, the above energy dips become energy gaps as shown in the inset to Fig. 3. Notice that in this example the transmission energy dips appear many times above the barrier height, that is, at energies well above the tunneling region.

One might be tempted to consider the newly formed transmission energy dips or gaps as a form of antiresonance, as used to describe transmission (or conductance) minima in quantum dots [20,21], quantum wires [22] or in quantum chaos [23,24]. Antiresonances, however, refer to zeros of the transmission amplitude whereas in our case, the transmission energy dips or gaps arise from a complex interference process involving many poles and residues in the expansion of the transmission amplitude given by Eq. (4), which has been studied in detail in Refs. [15,25]. Our findings may be of interest in studies on wave transport in one-dimensional disordered systems where transmission energy dips have been reported [26].

IV. DWELL TIME

The *dwell time* is defined according to the expression [2,27,28],

$$\tau_d(E) = \frac{1}{J_0}\int_0^L |\psi(x,E)|^2 dx, \tag{5}$$

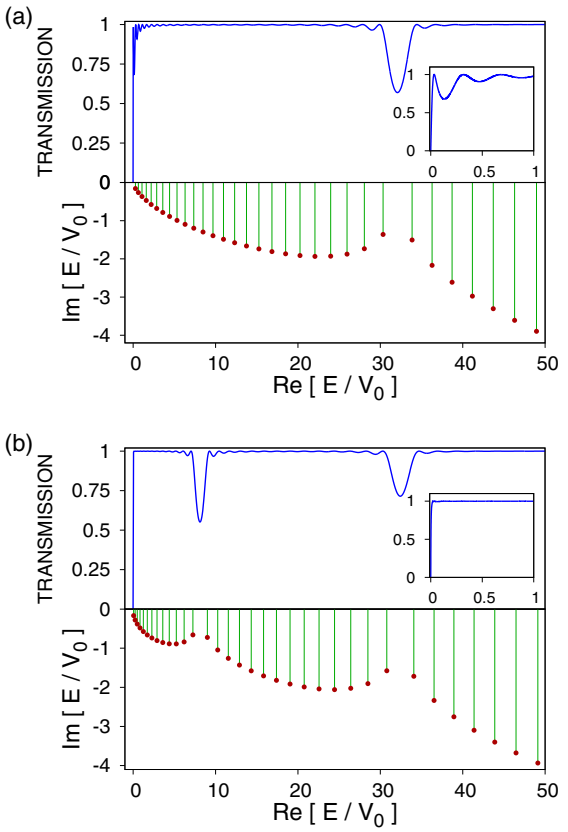

FIG. 7. (Color online) (a) The upper panel exhibits the transmission coefficient as a function of energy in units of the barrier height, for a multibarrier system formed by TIBBs which are separated by a parameter s having a depth $U_s = U_0$. One appreciates that the system ceases to be tunneling invisible and also the existence of an energy dip nearly 30 times above the barrier height. The lower panel shows the distribution of complex poles of the corresponding transmission amplitude $t(E)$. Here again as in Fig. 5, the lines joining the poles with the real energy axis are given to help the eye. They form a collar that distributes itself along the allowed energy region. (b) Refers to the case where the depths $U_s = 0$, which restores invisibility. The upper panel shows the apparition of a new energy dip corresponding, as shown in the lower panel, to a distribution of poles forming two collars. The insets in both figures above exhibit a zoom of the corresponding transmission coefficient in the energy range $0 < E/V_0 < 1$ (see text).

where $J_0 = (\hbar k)/m$ stands for the incoming flux. This quantity measures the amount of time that the incident particle spends within the internal region L of the potential. One may write it in units of $\tau_0 = L/J_0$, the time it takes for a free particle to traverse the distance L, and express it as [29,30]

$$\frac{\tau_d}{\tau_0} = \frac{1}{L}\int_0^L |\psi(x,E)|^2 dx = T + \frac{1}{L}[T\dot{\theta} + R\dot{\phi}] + \frac{R^{1/2}}{kL}\sin\phi, \tag{6}$$

where R stands for the reflection coefficient, $\dot{\theta}$ and $\dot{\phi}$ refer, respectively, to the so-called transmission and reflection times, the dot representing the derivative with respect to k of

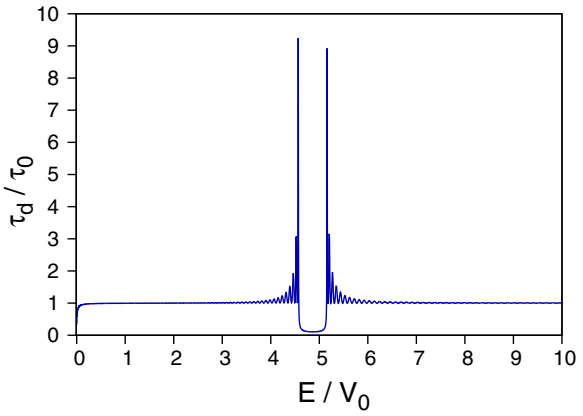

FIG. 8. (Color online) The dwell time τ_d for a multibarrier-tunneling invisible system with $N_{BB} = 100$ TIBBs with parameters as given on the text, in units of the time $\tau_0 = L/J_0$ that it takes for a particle to traverse the distance L, which corresponds to the total length of the system, and $J_0 = \hbar k/m$ refers to the free incoming flux. Notice that near the dip around $E/V_0 = 5$, the dwell time exhibits an oscillatory behavior which is particularly large at the dip edges (see text).

the phases θ and ϕ of the corresponding transmission, and reflection amplitudes $\mathbf{t}(k)$ and $\mathbf{r}(k)$.

For multibarrier resonant tunneling systems, near each resonant peak in an energy miniband, it is well known that the *dwell time* exhibits a Breit-Wigner shape, which implies that $\tau_d \gg \tau_0$ [1,28] and hence it will not be further considered here.

Figure 8 exhibits a plot of $\tau_d(E)$ as a function of the energy in units of the potential height V_0 for a chain of $N_{BB} = 100$ TIBBs with $s_0 = 2b_0$ and parameters: barrier heights $V_0 = 0.2$ eV, barrier widths $b_0 = 4.0$ Å, well depth $U_0 = -0.2$ eV, and well width $w_0 = 8$ Å. Notice that the barrier heights and the well depth are larger than for the system discussed previously. The exact numerical calculation of $\tau_d(E)$ is obtained by integrating the probability density along the internal region of the potential using the transfer matrix method. One sees that, except at very small energies and energies around the energy dip near $E/V_0 = 5$, $\tau_d(E)$ is very close to $\tau_0(E)$. The above result implies that the sum of the last two terms on the right-hand side of Eq. (6) adds to a vanishing contribution, although each term by itself may not be small. One sees, therefore, that except around the energies mentioned above, the time that the tunneling particle spends within the internal region of the potential is indistinguishable from that of a free evolving particle.

V. CONCLUDING REMARKS

It is worth commenting that tunneling invisibility holds in multibarrier systems by choosing the inter-building-block distance within a range of appropriate values, as displayed in Fig. 2, and also that by choosing appropriately that distance, one may control the energy range where the energy dips or gaps will occur, which may even include the tunneling region. Explaining the origin of the complex starlike patterns exhibited by Fig. 2 near the border of unity transmission may require using different techniques, may be similar as those employed in the description of the onset to chaos [31]. This deserves to be further studied. It is worth pointing out also the optic analog of the vanishing transmission phase in multibarrier-tunneling invisible systems with zero phase delay in negative-refractive-index photonic crystal superlattices [32,33], which might be of interest also to investigate. Finally, we would like to mention that our results depend on general analytical properties of the transmission amplitude for coherent processes and may open the way to the design, experimental scrutiny, and applications of these quantum systems.

ACKNOWLEDGMENTS

S.C. acknowledges a postdoctoral fellowship from CONACyT-México under Project No. 101541 and G.G.-C. acknowledges the partial financial support of UNAM-DGAPA-PAPIIT IN111814.

[1] G. García-Calderón and A. Rubio, Phys. Rev. A **55**, 3361 (1997).
[2] R. Landauer and T. Martin, Rev. Mod. Phys. **66**, 217 (1994).
[3] P. Kurasov and A. Lunger, Lett. Math. Phys. **73**, 109 (2005).
[4] S. P. Maydanyuk, Ann. Phys. (NY) **316**, 440 (2005).
[5] A. A. Stahlhofen, Phys. Rev. A **51**, 934 (1995).
[6] G. A. Kerimov and A. Ventura, J. Math. Phys. **47**, 082108 (2006).
[7] L. D. Landau and E. M. Lifshitz, *Quantum Mechanics* (Pergamon Press, Oxford, 1977), Sec. 25.
[8] S. Cordero and G. García-Calderón, Phys. Rev. A **79**, 052103 (2009).
[9] S. Cordero and G. García-Calderón, Phys. Rev. A **88**, 052118 (2013).
[10] S. Longhi, Phys. Rev. A **82**, 032111 (2010).
[11] D. K. Ferry and S. M. Goodnick, *Transport in Nanostructures* (Cambridge University Press, Cambridge, 1997).
[12] G. Bastard, *Wave Mechanics Applied to Semiconductor Heterostructures* (Halsted Press, Sydney, 1988).
[13] R. G. Newton, *Scattering Theory of Waves and Particles*, 2nd ed. (Dover Publications, Mineola, 2002), Chap. 12.
[14] E. Jüli and D. Mayers, *An Introduction to Numerical Analysis* (Cambridge University Press, Cambridge, 2003).
[15] S. Cordero and G. García-Calderón, J. Phys. A: Math. Theor. **43**, 185301 (2010).
[16] R. M. More, Phys. Rev. A **4**, 1782 (1971).
[17] G. García-Calderón, R. Romo, and A. Rubio, Phys. Rev. B **56**, 4845 (1997).
[18] S. Cordero and G. García-Calderón, J. Phys. A **44**, 305302 (2011).
[19] G. García-Calderón and R. E. Peierls, Nucl. Phys. A **265**, 443 (1976).
[20] P. A. Orellana, F. Domínguez-Adame, I. Gómez, and M. L. Ladrón de Guevara, Phys. Rev. B **67**, 085321 (2003).
[21] Z. Z. Sun, R. Q. Zhang, W. Fan, and X. R. Wang, J. Appl. Phys. **105**, 043706 (2009).

[22] W. Porod, Z.-a. Shao, and C. S. Lent, Phys. Rev. B **48**, 8495 (1993).
[23] C. Zhang, J. Liu, M. G. Raizen, and Q. Niu, Phys. Rev. Lett. **92**, 054101 (2004).
[24] I. Dana and D. L. Dorofeev, Phys. Rev. E **72**, 046205 (2005).
[25] S. Cordero and G. García-Calderón, J. Phys. A: Math. Theor. **43**, 415303 (2010).
[26] M. Díaz, P. A. Mello, M. Yépez, and S. Tomsovic, Europhys. Lett. **97**, 54002 (2012).
[27] F. T. Smith, Phys. Rev. **118**, 349 (1960).
[28] M. Büttiker, Phys. Rev. B **27**, 6178 (1983).
[29] E. H. Hauge, J. P. Falck, and T. A. Fjeldly, Phys. Rev. B **36**, 4203 (1987).
[30] G. García-Calderón and A. Rubio, Solid State Commun. **71**, 237 (1989).
[31] F. Baldovin and A. Robledo, Phys. Rev. E **66**, 045104 (2002).
[32] S. Kocaman, M. S. Aras, P. Hsieh, J. F. McMillan, C. G. Biris, N. C. Panoiu, M. B. Yu, D. L. Kwong, A. Stein, and C. W. Wong, Nature Photon. **5**, 499 (2011).
[33] J. Schilling, Nature Photon. **5**, 449 (2011).